



Article

Study of the Influence of the Thermal Capacity of the Lining of Acid Melting Furnaces on Their Efficiency

Viktor Alekseevich Kukartsev ¹, Vladislav Viktorovich Kukartsev ^{2,3,4}, Vadim Sergeevich Tynchenko ^{4,5,6,*} , Sergei Olegovich Kurashkin ^{4,6,7} , Roman Borisovich Sergienko ⁸, Sergei Vasilievich Tynchenko ^{9,10}, Ilya Alexandrovich Panfilov ^{4,11,12}, Svetlana Vitalievna Ereemeeva ⁷ and Tatyana Aleksandrovna Panfilova ⁵

- ¹ Department of Materials Science and Materials Processing Technology, Polytechnical Institute, Siberian Federal University, 660041 Krasnoyarsk, Russia
 - ² Department of Informatics, Institute of Space and Information Technologies, Siberian Federal University, 660041 Krasnoyarsk, Russia
 - ³ Department of Information Economic Systems, Institute of Engineering and Economics, Reshetnev Siberian State University of Science and Technology, 660037 Krasnoyarsk, Russia
 - ⁴ Digital Material Science: New Materials and Technologies, Bauman Moscow State Technical University, 105005 Moscow, Russia
 - ⁵ Department of Technological Machines and Equipment of Oil and Gas Complex, School of Petroleum and Natural Gas Engineering, Siberian Federal University, 660041 Krasnoyarsk, Russia
 - ⁶ Information-Control Systems Department, Institute of Computer Science and Telecommunications, Reshetnev Siberian State University of Science and Technology, 660037 Krasnoyarsk, Russia
 - ⁷ Laboratory of Biofuel Compositions, Siberian Federal University, 660041 Krasnoyarsk, Russia
 - ⁸ Machine Learning Department, Gini GmbH, 80339 Munich, Germany
 - ⁹ Department of Digital Control Technologies, Institute of Business Process Management, Siberian Federal University, 660041 Krasnoyarsk, Russia
 - ¹⁰ Department of Computer Science and Computer Engineering, Institute of Computer Science and Telecommunications, Reshetnev Siberian State University of Science and Technology, 660037 Krasnoyarsk, Russia
 - ¹¹ Department of Systems Analysis and Operations Research, Reshetnev Siberian State University of Science and Technology, 660037 Krasnoyarsk, Russia
 - ¹² Department of Business Informatics and Business Process Modeling, Siberian Federal University, 660041 Krasnoyarsk, Russia
- * Correspondence: vadimond@mail.ru; Tel.: +7-95-0973-0264



Citation: Kukartsev, V.A.; Kukartsev, V.V.; Tynchenko, V.S.; Kurashkin, S.O.; Sergienko, R.B.; Tynchenko, S.V.; Panfilov, I.A.; Ereemeeva, S.V.; Panfilova, T.A. Study of the Influence of the Thermal Capacity of the Lining of Acid Melting Furnaces on Their Efficiency. *Metals* **2023**, *13*, 337.
<https://doi.org/10.3390/met13020337>

Academic Editor: Chenguang Bai

Received: 30 November 2022

Revised: 2 February 2023

Accepted: 3 February 2023

Published: 8 February 2023



Copyright: © 2023 by the authors. Licensee MDPI, Basel, Switzerland. This article is an open access article distributed under the terms and conditions of the Creative Commons Attribution (CC BY) license (<https://creativecommons.org/licenses/by/4.0/>).

Abstract: First of all, the smelting equipment is the most important component of a foundry's main production process and therefore requires constant reproduction. This is ensured by timely and high-quality maintenance and repair, the cost of which is 8–12% of the total costs. The technical and economic conditions of the enterprise itself depend on this, as the productivity of workers during production is directly related to the technical condition of the equipment and its downtime for repairs. An important factor in ensuring a melting furnace's reproduction is a replacement of the worn lining, which leads to downtime of the smelting furnace and reduces the efficiency of its operation. The amount of torque required depends directly on the compound used. The quality of the manufacturing and sintering process of the lining, which provides the necessary durability, is affected by the heat capacity of the materials used when they are affected by the melting temperature of the alloys. In the present work, using the BRUKER D8 ADVANCE diffractometer, the Shimadzu XRF-1800 spectrometer and the STA 449 F1 Jupiter synchronous thermal analyzer, we probed the changes in the heat capacity of quartzite and PKMVI-3 under the action of temperatures of 200–1550 °C. This technology allows the manufacture of a lining that maintains high stability during operations at 1550–1600 °C melting modes.

Keywords: induction furnace; synthetic iron; quartzite; lining; alloy smelting; heat capacity; melting furnace operation efficiency

1. Introduction

The manufacturing of castings is the most common process in forming part blanks due to its low cost and versatility of application. It makes it possible to obtain workpieces as close as possible to the profile of the future part and provide the necessary requirements for mechanical, physical, technical and special properties that are specified in the technical conditions [1]. This process can be applied to both individual and mass production. As of 2020, in Russia, various alloys and smelting equipment have been used for the production of castings, as shown in Figure 1.

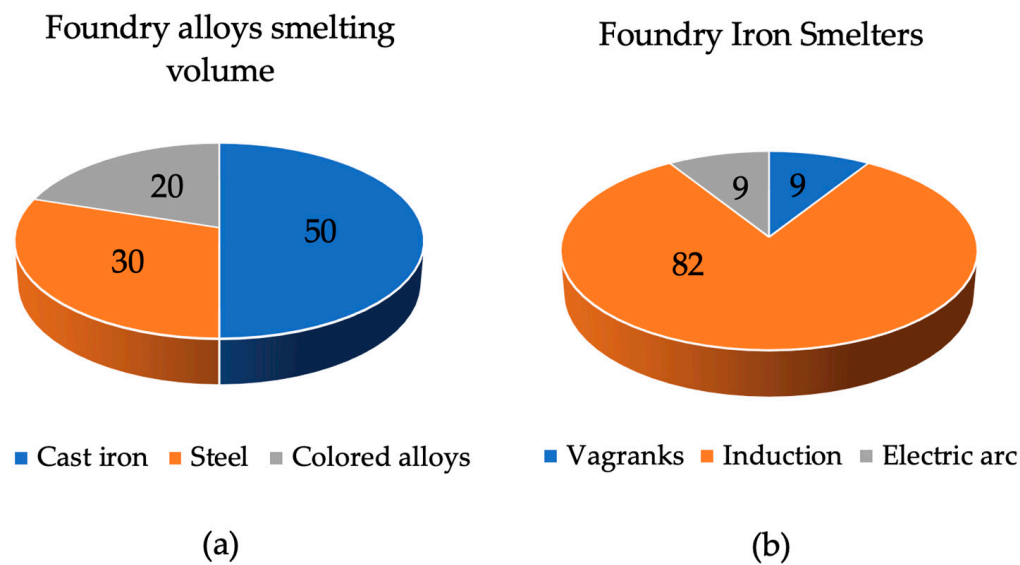


Figure 1. Distribution of foundries.

Cast iron is the most common alloy, and induction furnaces are the most common furnace. Of the total number of induction crucible furnaces, about 18% are high-frequency induction furnaces designed for smelting alloy steel, and the rest are medium-frequency furnaces that can be used for smelting any alloy. The bulk of these are industrial-frequency induction crucible furnaces (ICFs), which have been in use since the middle of the last century [2–4].

First of all, the smelting equipment is the most important component of the foundry's production base and requires constant reproduction. For this reason, a great deal of attention is being paid to improving the use of fixed assets, primarily related to the growth of return funds through improving the utilization of the equipment, improving the structure of fixed assets, modernization through improving the equipment and technology, and implementation of organizational and technical measures [5]. An important aspect of ensuring the functionality of a melting furnace is to replace the worn lining. Therefore, increasing the reliability of the smelter is one of the main tasks that ensures the necessary degree of reproduction of the main production facilities in order to comply with the following parameters of the aggregate: versatility in smelting alloys, performance, high lining durability, energy efficiency and maintenance costs [6]. Increased efficiency in the use of equipment is ensured by the adoption of new technologies that reduce downtime and reduce material inputs. The quality of the manufacturing process and the sintering of the lining affects its durability and, consequently, the efficiency of the melting furnace.

The main purpose of induction furnaces is the smelting of synthetic iron based on the use of scrap steel in the form of sheet trimmings, shavings and other metal waste with a small volume and weight. Figure 2 shows an image of an induction furnace at the moment of loading, with the main components labeled.

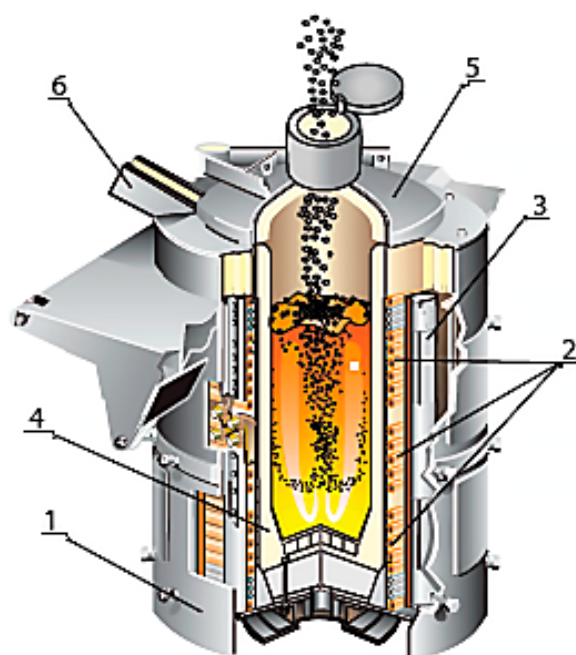


Figure 2. Induction melting furnace: 1—drain sock; 2—furnace cover; 3—gas atmosphere; 4—scrap metal; 5—inductor; 6—case.

To make the furnace lining, the designers intended to use an acidic quartzite-based lining as the cheapest option, as its price is four–six times lower than the basic and neutral equivalents. The operation of these furnaces proved to be very robust, namely, 300–350 melts. The smelting of synthetic pig iron in these furnaces reduces its cost by 25–39% compared with the secondary smelting of iron [7–9]. This is particularly relevant in the current context, where all countries are facing the effects of the pandemic and the ensuing energy crisis [10].

The use of quartzite in the composition of refractory masses began in the second half of the 18th century for the manufacture of dyno products, which consisted of the linings of various heating and smelting furnaces [11–14]. Different types of quartzite differ in their mineral composition and content of elemental impurities (especially manganese, iron, aluminum, titanium, boron and phosphorus), the presence and concentration of which determine their industrial application and the possibility of further enrichment [15–18].

To obtain a lining with a high stability, it is necessary to use quartzite with a minimal number of impurities and a humidity of no more than 0.3%. However, manufacturers use wet enrichment to remove impurities. This includes washing operations, scrubbing, gravity, magnetic separation and flotation, resulting in a humidification of up to 2–3%. Therefore, the preparation of the lining of the induction furnace requires pre-drying with a further generation of the tridymite and cristobalite phases [19–22]. The tridymite produced during the drying of the quartzite and the subsequent sintering of the lining has been shown to maintain a constant volume at 840–1470 °C for a long time and thus provides the lining with a high resistance.

Based on the specificity conditions of service, the following basic requirements apply to the lining of the induction tiger furnaces, which are set out in the work [23].

When these requirements are met, three layers are formed in the lining after sintering, as shown in Figure 2.

Despite the fact that during the drying and sintering process the refractory materials undergo significant changes in their properties, after this process, the following three zones in the lining should be obtained: monolithic (sintered), semi-sintered and loose (Figure 3).

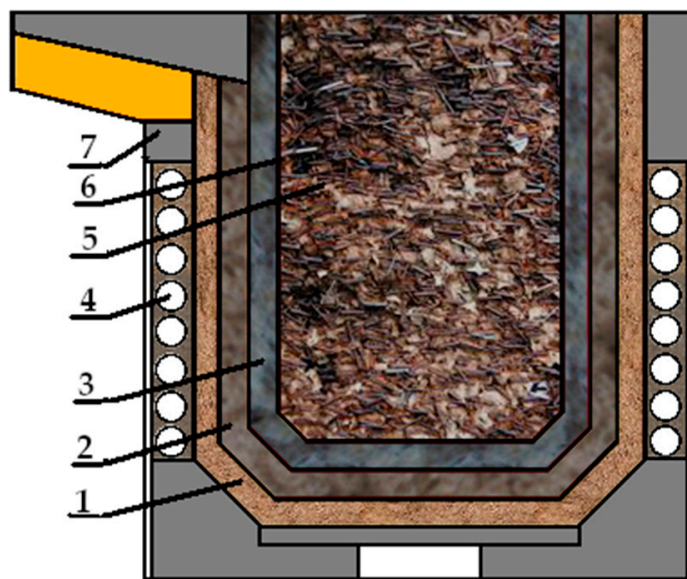


Figure 3. Scheme of the furnace indicating the zones of the lining: 1—the bulk layer; 2—the semi-welded layer; 3—the sintered layer; 4—the furnace inductor; 5—the metal load; 6—the polished layer; 7—the furnace body.

The boundaries of the transition from one zone to another are rather conventional, but in terms of their phase composition and thermophysical parameters, they all differ significantly from each other [24].

The phase composition of each zone is significantly influenced by the heat capacity of the formed elemental cells of the quartzite, which depend on the chemical and mineralogical composition of the initial material [25].

Traditional synthetic iron smelting technology requires a 30-degree liquid residue (bog) after discharge of 35% of the finished melting and melting temperatures not exceeding 1450 °C. The content limit of steel scrap is justified by its melting point since the melting point of carbon steel scrap is, depending on the chemical composition, 1400–1600 °C.

2. The Problem

At present, however, the situation in the market for cast iron castings has changed dramatically, as follows: cast iron scrap is virtually non-existent, and the cost of cast iron has increased dramatically, as has the cost of shipping it. This has led to the fact that synthetic cast iron can only be smelted in ICFs using increased amounts of steel scrap, carburizers and ferroalloys. However, to do this, it is necessary to raise the melting point above the allowable temperature for the furnace.

There is also a problem related to the persistence of the acid lining. The practice has shown that if the alloy is smelted at 1550 °C, the lining's resistance decreases to 180 melts [26]. Replacing the acidic lining with a basic or neutral lining that can withstand this temperature causes it to cost 4–6 times more. The use of finished liner masses is advisable in medium-frequency furnaces where the inductor is fixed and the lining is not deformed. In ICFs, it is free and deformed during cyclic smelting modes and has been shown to be able to grow up to 50 mm by the end of the cycle, despite the periodicity of the tightening pins tightening the inductor's turns. This type of deformation negatively affects the stability of the basic and neutral linings. In addition, the durability of the lining is affected by defects, which can be caused by a multitude of factors in its manufacture [27], sintering and slag mode [28]. This is influenced by the quality of the quartzite used and the manufacturing process of the lining mass.

As early as 1912, C. N. Fenner [29] established phase transformations in the quartzite when it was heated, in the form of a diagram scheme, according to which the tridymite

phase is first and then the cristobalite phase. This was reflected in other studies [30,31]. Later, many studies disproved this pattern, which was explained by the emergence of the method of X-ray and the development of physico-chemical methods in the final 60–70 years of the last century. For this reason, since 1961, in studies of the phase transformations of quartzite when heated, tridymite has not been detected [32–35]. Spiker proposed a variant of the modified SiO₂ diagram when heated to 1550 °C [36]. In addition, some studies have highlighted the regularity of the appearance of cristobalite first and then tridymite [37–42]. It was then established that the transformation to cristobalite begins at a prolonged temperature of 1000 °C, and at 1250–1450 °C, the process is intensified [43]. This process is also influenced by impurities in the source material [44]. Other studies have established the obligatory presence of a mineralizer to obtain the tridymite phase [45,46].

However, it must be considered that phase transformations occur with the release of heat and are accompanied by the emergence of a sparser aggregate state; that is, an increase in the volume and a reduction in the density due to the expansion of the crystal lattice [47]. In addition, phase transformations can be accompanied by both reductions in volume and heat release. The thermal stability of the melting furnace is estimated by the number of melts, and each melting (in the case of a 2.5 t furnace) is the heating of the lining after sintering to 1550 °C, then the melting mode occurs at 1550–1600 °C, and the temperature drops to 1450–1470 °C to drain the first portion of the alloy. After this, the second batch of metal is drained; during this time, the temperature of the lining layer is released when draining the first batch of metal reaches 1025 °C. After all the metal has been drained, the fresh metal filling is loaded, and the temperature of the lining is 800–900 °C. Everything is repeated until the lining has been completely worn. Under these conditions, changes in the structure of the quartzite are significantly influenced by the heat capacity of the initial material used, which is directly dependent on the resulting phase state.

The quantitative content of the different phases in the quartzite, when exposed to the repeated heating and cooling temperatures necessary for melting, affects the heat capacity of the lining itself and its durability.

Therefore, the study of changes in the heat capacity of the quartzite, which affects the stability of the applied lining when the melting temperatures are above 1450 °C, is an urgent task.

3. Materials and Methods

The study was carried out for quartzite (PKMVI-3V brand), with a humidity of 3.5%, supplied by JSC “DINUR”. According to the supplier, the finished product mainly contains quartz but also includes impurities of chalcedony, carbonates, opals and clay minerals, with a low concentration of iron oxides and high dispersion. The company, according to TU 1511-022-00190495-2003, guarantees the chemical composition presented in Table 1 (the contents of the remaining impurities are not given). In addition, the following grain composition is guaranteed, in mass proportions: remaining on grid No. 2, 6–15 inclusive; remaining on grid No. 3.2, not more than 5; passing through grid No. 0.5, 50–59 inclusive; passing through grid No. 0.1, 31–41.

Table 1. Chemical composition of PKMVI-3B quartzite.

Chemical Composition of PKMVI-3B Quartzite	Content (%)									
	SiO ₂	Al ₂ O ₃	CaO	MgO	TiO ₂	Fe ₂ O ₃	P ₂ O ₅	MnO	Na ₂ O	K ₂ O
According to TU	97.5	1.1	-	-	-	0.6	-	-	-	-
Spectrometry of material dried at 200 °C	96.54	0.982	0.189	0.025	0.205	0.93	0.014	0.031	0.105	0.374

The Shimadzu XRF-1800 X-ray fluorescence spectrometer (Shimadzu, Japan) was used to determine the chemical composition. The device was equipped with collimators and a built-in digital camera. The rotation speed of the sample was 60 rev/min.

Phase composition studies were carried out using the BRUKER D8 ADVANCE diffractometer (Bruker, Germany). The copper anode X-ray tube was used, and the diffraction spectrum was recorded by the VÅNTEC-1 high-speed positional detector.

The STA 449 F1 Jupiter (NETZSCH, Germany) was used for thermal analysis of the quartzite.

Earlier studies of changes in the structure of the quartzite at different temperatures used to remove the moisture in the original material showed their influence on the formation of phases under the influence of the temperatures necessary for sintering the lining [48]. For this reason, the following research methodology was adopted:

- We determined the chemical composition of the quartzite, taking the presence of concomitant impurities into account;
- The raw quartzite portion was heated to a temperature of 800 °C, given an exposure of 1 h and cooled to room temperature, then subjected to subsequent heating with exposure at each test point to remove the card and determine the parameters of the crystal lattice at uniform temperatures suitable for sintering and operating melting;
- The next batch of raw quartzite was heated to a temperature of 200 °C, given an exposure of 1 h and cooled to room temperature. We then performed the same heating mode as in Step 2;
- We investigated the change in the heat capacity of the quartzite using different moisture removal technologies (as in Steps 2 and 3), followed by heating corresponding to the sintering temperatures of the lining and several melting cycles.

The temperatures selected for this study were based on the following:

- Between 200 and 800 °C, the approximate temperature for removing free moisture;
- 600 °C, intensive phase conversion with heat release, applied during operation [49];
- 1550–1600 °C, melting mode, for carburizing, alloying and modifying operations;
- 1450–1470 °C, first alloy discharge;
- 1025 °C, temperature of the released lining layer after the first discharge (at this time the second portion of the alloy is drained);
- 800–900 °C, the temperature of the lining after discharging all the metal, when fresh metal filling is loaded.

4. Results and Discussion

Since the process of phase formation under temperature is affected by the number of impurities in the quartzite itself, the chemical composition of the quartzite was first analyzed using the Shimadzu XRF-1800X-ray fluorescent wave dispersion spectrometer. As a result of this analysis, it was found that the quantity of SiO₂ was 96.54% instead of 97.5%, the quantity of Al₂O₃ was 0.982% instead of 1.1%, the CaO content was 0.189% instead of 0.089%, and Fe₂O₃ amounted to 0.93%, which is significantly more than declared, and the number of uncharged impurities was 0.638%. The results of the analysis are shown in Table 1.

The study of changes in the structure of the quartzite was carried out with the BRUKER D8 ADVANCE diffractometer, equipped with a Bragg–Brentano focus and an HTK 16 high-temperature chamber. The imaging took place at the angles of $2\Theta = 10\text{--}90^\circ$ in increments of 0.007; the duration of the imaging was 1 h.

Figure 4 shows the structure of a quartzite lattice at 1550 °C, pre-treated to remove moisture at 800 °C.

The diffractogram of quartzite pre-treated at 200 °C and subsequently heated to 1550 °C is shown in Figure 5.

To decipher the results of the study of the changes in the structure of the quartzite, the available databank was used in the form of cards of elementary cells with their characteristics (Table 2).

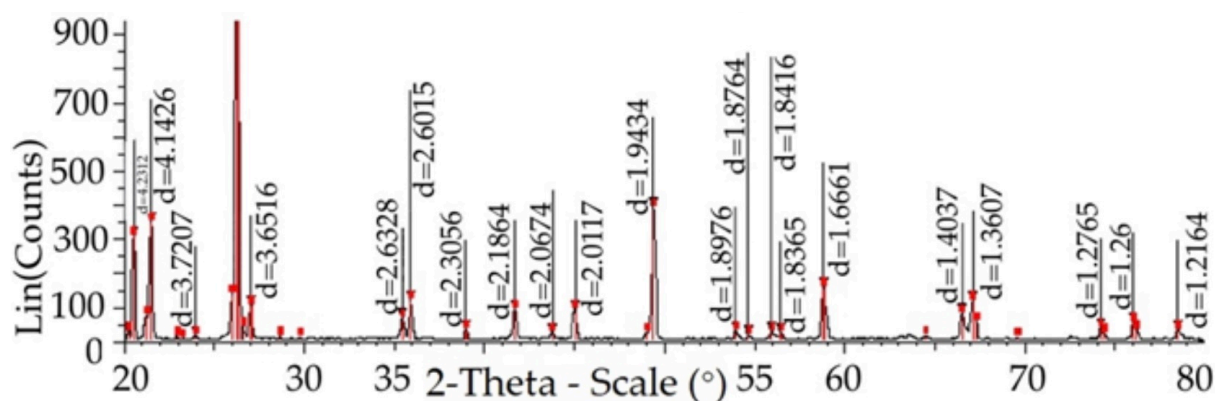


Figure 4. The structure of the quartzite consists of elementary cells of cristobalite, marked with purple color (card 01-085-0621); tridymite, marked with yellow (card 00-018-1170) and cells of quartzite, marked in red (card 01-071-0911).

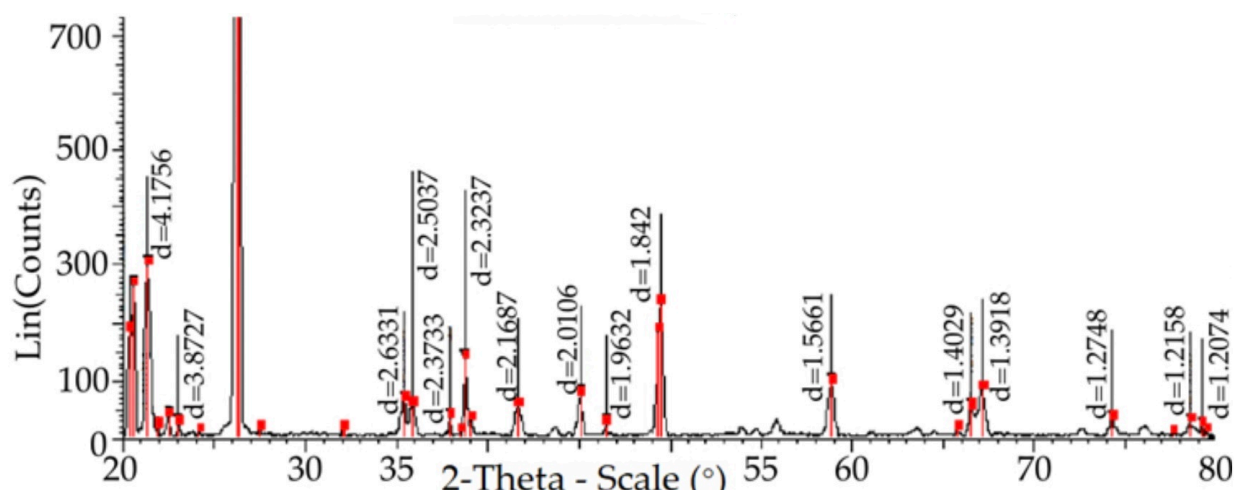


Figure 5. The structure of quartzite consists of elementary cells of cristobalite (colored purple, cards 00-011-0695) and quartzite (colored red, cards 01-071-0911).

Table 2. Characteristics of elementary cell cards used in the research process.

Indicators	No.									
	00-012-0708	01-071-0911	00-005-0490	01-083-2187	01-070-7344	02-002-0278	01-011-0695	01-085-0621	01-071-0032	00-018-1170
a (Å)	4.994	5	4.913	4.965	4.915	7.12	4.971	7.16	18.494	18.504
b (Å)	5.438	5.49	5.405	5.424	5.406	-	-	-	4.991	5.006
Mol. weight (g/mol)	60.08	52.87	60.08	60.08	60.08	60.08	60.08	60.08	60.08	60.08
Volume (Å ³)	117.45	118.86	112.98	115.79	113.09	360.94	170.95	367.06	2110.15	2215.08
D _x (g/cm ³)	2.548	2.216	2.649	2.58	2.647	2.211	2.335	2.174	2.270	2.254
c (Å)	-	-	-	-	-	-	-	-	26.832	23.845

The parameters of the changes in the structure of the quartzite that occurred during the rise of the set temperatures were determined as follows. All the diffractograms taken counted the total number of crystalline phases, the content of which was not less than 5% and 100% were selected. The fraction of each crystalline phase was then determined, and its mean values were calculated, where d_{avg} is the average intergloss distance, D_{avg} is the

average density, V_{avg} is the average volume and M_{avg} is the average molecular mass of the lattice.

The results of the average characteristics of the parameters of the quartzite (including the phase composition) exposed to different temperatures for the removal of moisture and at the temperatures specified in the study are presented in Table 3.

Table 3. Average parameters and phase composition of the quartzite crystal lattice.

Lattice Parameter	Temperature (°C)						
	25/30 Dry	200	600	870	1000	1470	1550
d_{avg} (Å)	2.814/ 2.7574	2.8340/ 2.9012	2.7913/ 3.0066	2.9277/ 3.0545	2.9796/ 3.1048	3.0384/ 3.156	3.2619/ 3.2156
V_{avg} (Å ³)	119.1/ 114.83	116.55/ 115.41	117.47/ 647.47	125.86/ 1653.02	124.06/ 1722.83	124.04/ 1742.69	143.65/ 1606.96
D_{avg} (g/cm ³)	2.5971/ 2.601	2.552/ 2.592	2.333/ 2.502	2.292/ 2.2685	2.291/ 2.266	2.229/ 2.265	2.227/ 2.258
M_{avg} (g/mol)	60.08/ 60.08	60.08/ 60.08	55.16/ 60.08	53.91/ 58.38	53.66/ 58.63	53.66/ 58.79	54.41/ 58.79
Phase composition	Quartzite	Quartzite	Quartzite/ tridymite quartzite	Quartzite cristobalite/ tridymite quartzite	Quartzite cristobalite/ tridymite quartzite	Quartzite cristobalite/ tridymite quartzite	Quartzite cristobalite/ tridymite cristobalite Quartzite

In the numerator, values are given for quartzite treated at 200 °C; the denominator gives the values for quartzite treated at 800 °C. d_{avg} is the average interval–skeleton distance, D_{avg} is the average density, V_{avg} is the average volume and M_{avg} is the average molecular mass of the grid.

The study of changes in the thermal capacity of quartzite was carried out on the NETZSCH STA 449C Jupiter instrument during thermal analysis. The heating rate was 10 K/min, and the collection speed of the points was 100 p/min. Two corundum crucibles were used for the measurements, one of which contained an experimental specimen and the other was used as a reference. High measurement accuracy ensured the maximum uniform distribution of the examined material in the crucible [50].

The aim was to study changes in the heat capacity of the quartzite at the temperatures experienced by the lining during the melting cycles immediately after the sintering process (three melting cycles were investigated). As a result, the thermograms were obtained (Figures 6 and 7).

The heat capacity values are summarized in Table 4.

Table 4. Heat capacity (ΔC_p) values of quartzite at the operating temperatures of melting cycles: No. 1, quartzite treated at 200 °C; No. 2, quartzite treated at 800 °C J/K.

Specific Heat (ΔC_p)	Temperature (°C)																	
	1550	1470	1025	870	1025	1470	1550	1470	1025	870	1025	1470	1550	1470	1025	870	1025	1470
Quartzite No. 1 (J/K)	0.018	0.014	0.015	0.024	0.023	0.03	0.007	0.002	0.010	0.015	0.040	0.019	0.015	0.012	0.035	0.020	0.022	0.022
Quartzite No. 2 (J/K)	0.009	0.017	0.037	0.035	0.037	0.033	0.018	0.009	0.024	0.044	0.050	0.031	0.022	0.014	0.020	0.045	0.025	0.029

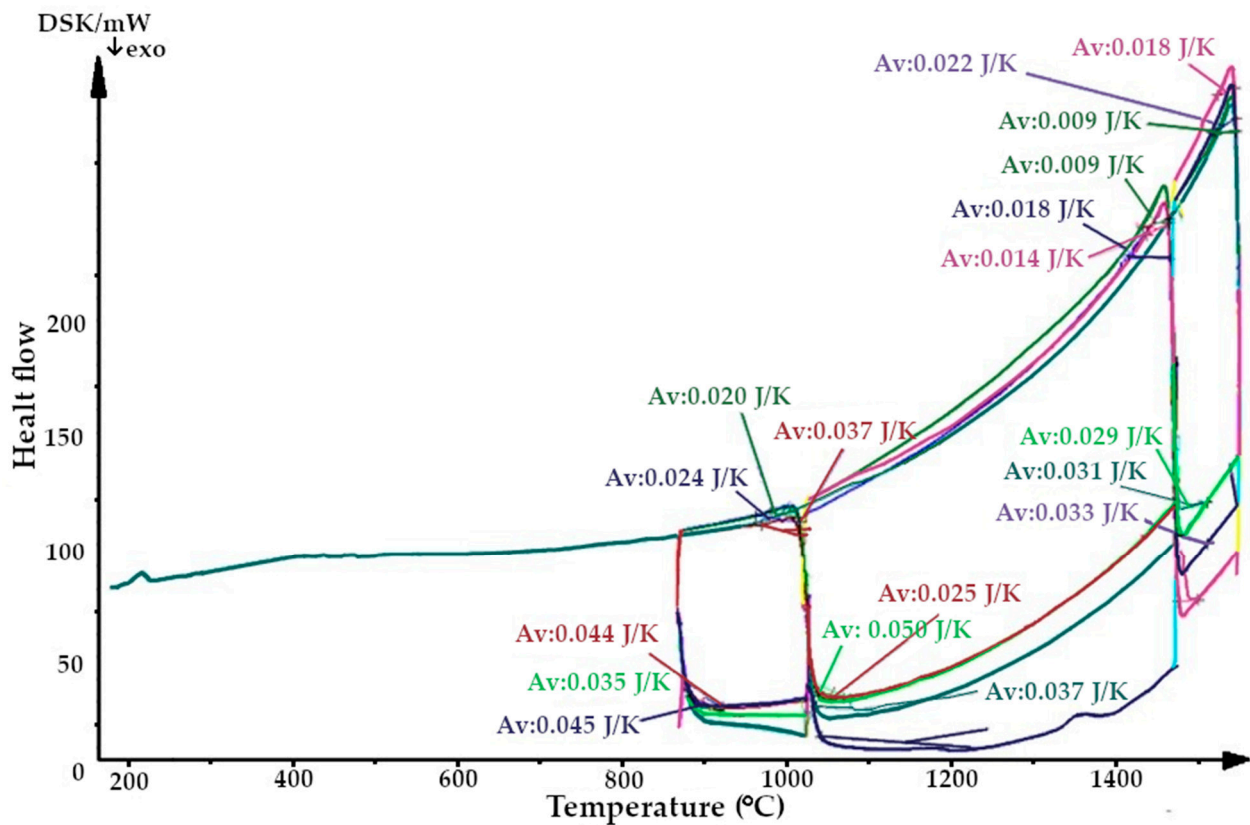


Figure 6. Thermogram of quartzite, calcified at 800 °C (Av, average heat capacity).

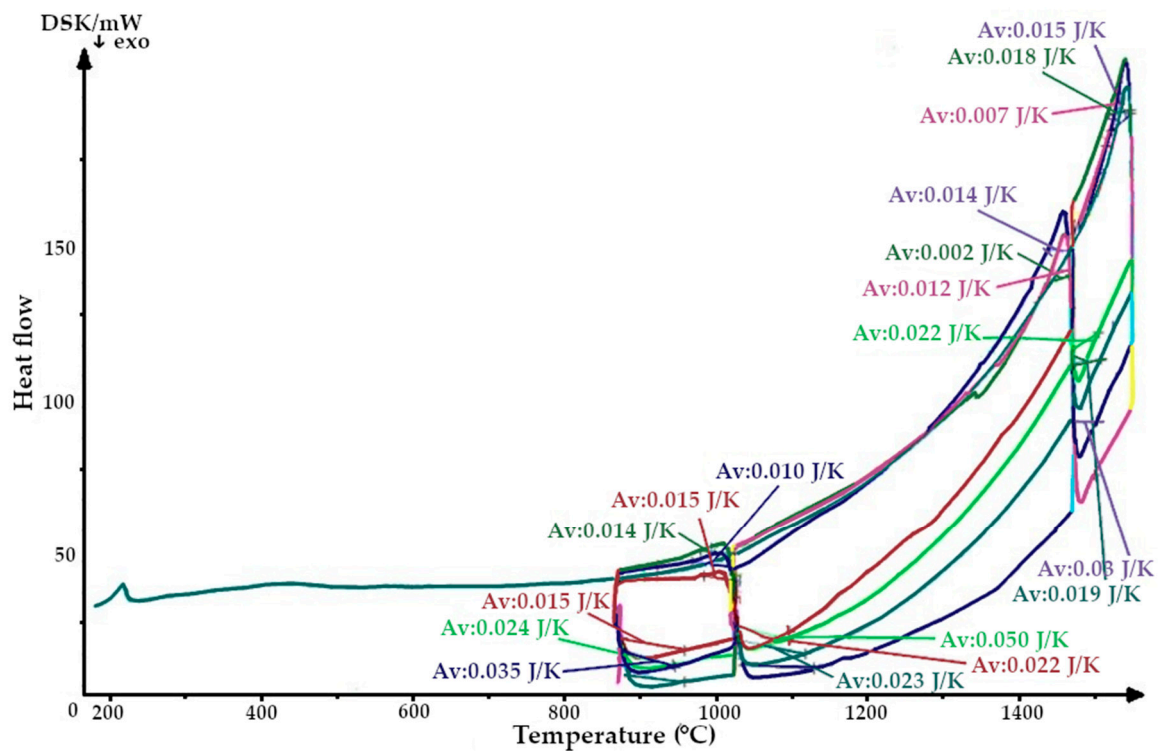


Figure 7. Thermogram of a quartzite, calcified at 200 °C and sintered with an induction furnace's lining.

Using the values shown in Table 4, the heat capacity of the quartzite was plotted as shown in Figure 8.

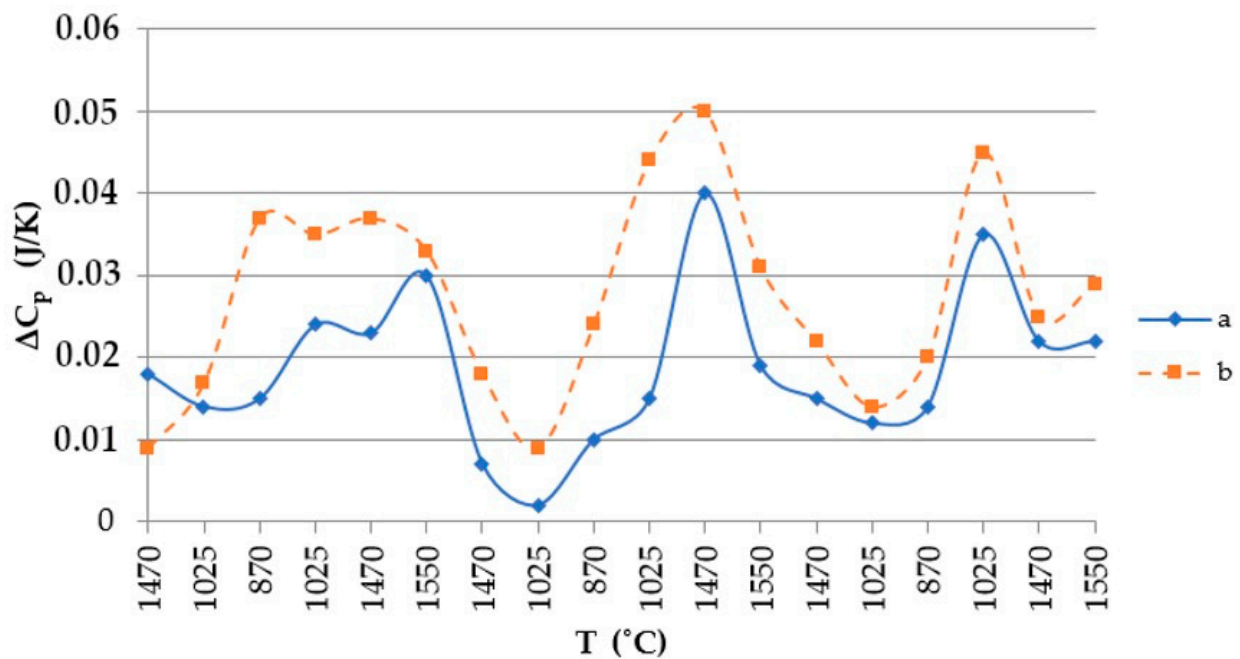


Figure 8. Thermal temperature dependence graph: a, quartzite treated at 200 °C; b, quartzite treated at 800 °C.

The values of the heat capacity in each melting cycle were selected, and graphs of their changes were constructed. These are presented as fragments of thermograms in Figures 9–14 for each type of quartzite.

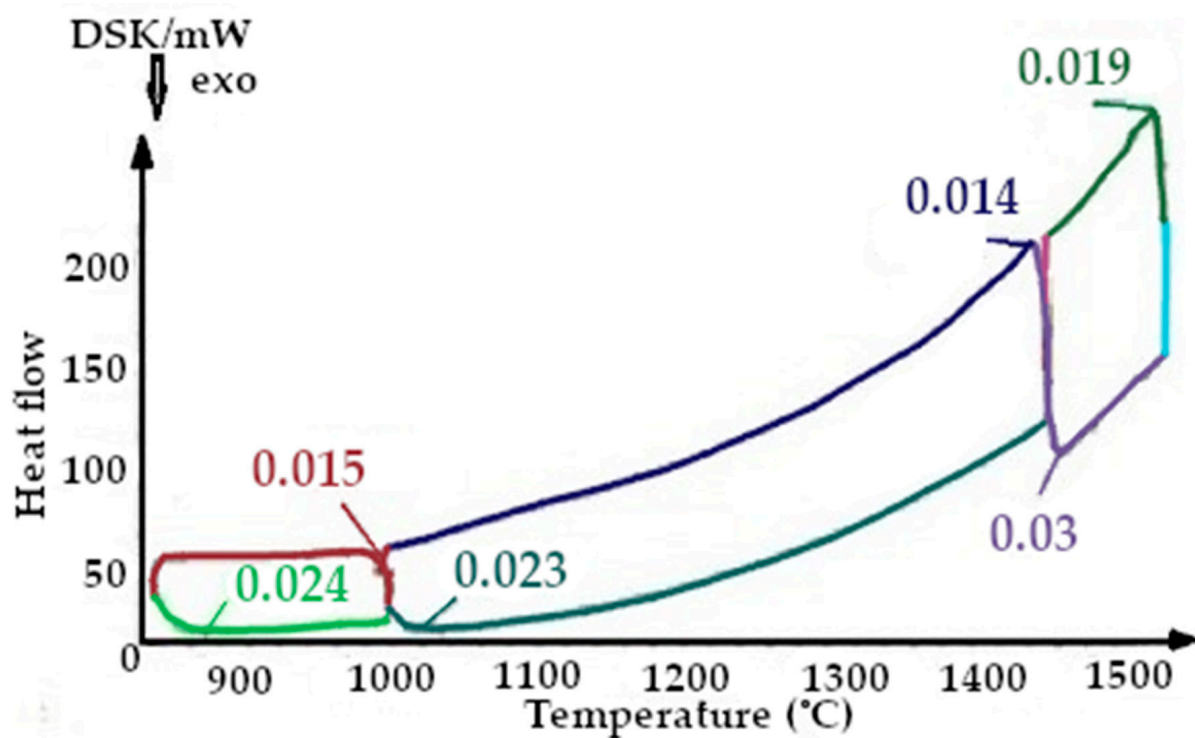


Figure 9. Fragment of the thermogram of quartzite, calcified at 200 °C (Cycle 1), where: ■—cooling up to 1470 °C, ■—heating up to 1025 °C, ■—cooling up to 870 °C, ■—cooling up to 1550 °C, ■—drainage at 1470 °C, ■—heating up to 1470 °C, ■—heating up to 1550 °C, ■—drainage at 1550 °C.

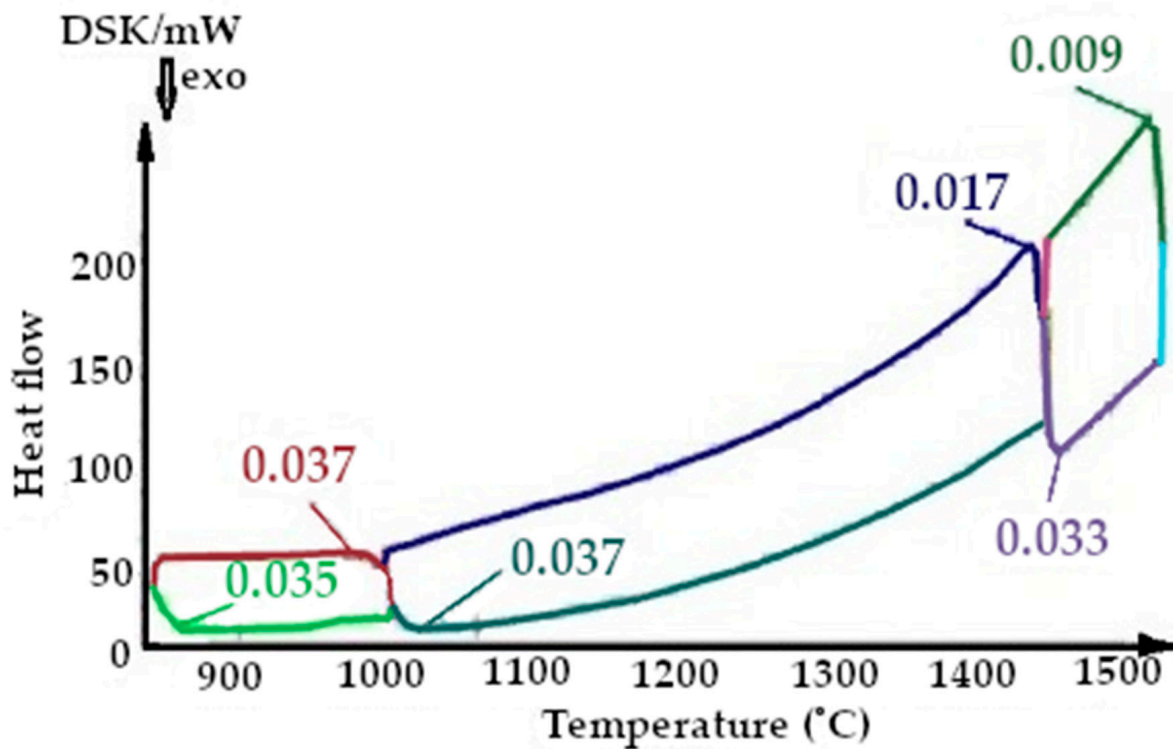


Figure 10. Fragment of the thermogram of quartzite, calcified at a temperature of 200 °C (Cycle 1), where: ■—cooling up to 1470 °C, ■—heating up to 1025 °C, ■—cooling up to 870 °C, ■—cooling up to 1550 °C, ■—drainage at 1470 °C, ■—heating up to 1470 °C, ■—heating up to 1550 °C, ■—drainage at 1550 °C.

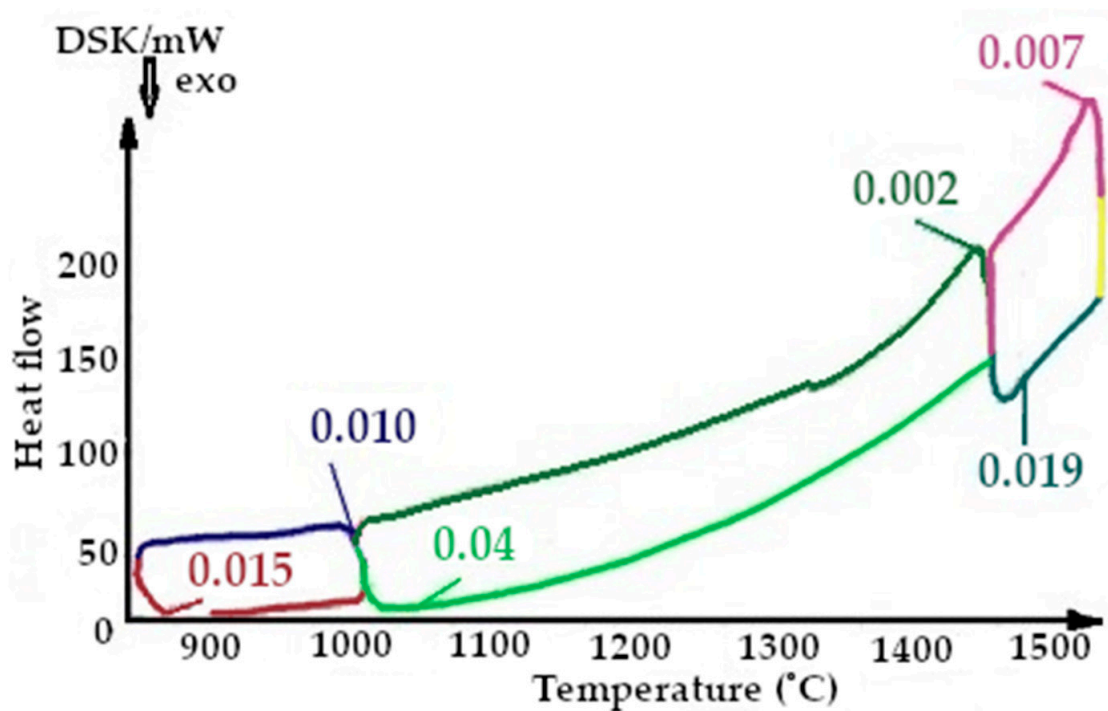


Figure 11. Fragment of the thermogram of quartzite, calcified at a temperature of 200 °C (Cycle 2), where: ■—cooling up to 1550 °C, ■—drainage at 1470 °C, ■—cooling up to 1470 °C, ■—cooling up to 870 °C, ■—heating up to 1025 °C, ■—heating up to 1550 °C, ■—heating up to 1470 °C.

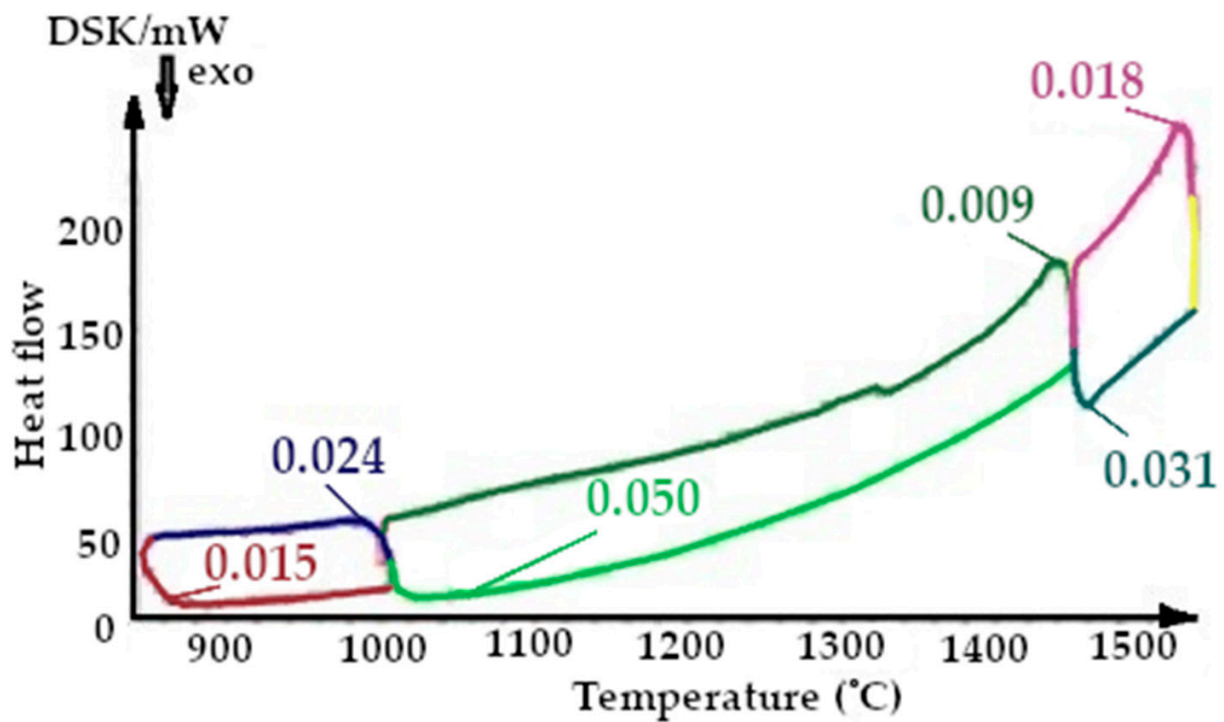


Figure 12. Fragment of the thermogram of quartzite, calcified at a temperature of 800 °C (Cycle 2), where: —cooling up to 1550 °C, —drainage at 1470 °C, —cooling up to 1470 °C, —cooling up to 870 °C, —heating up to 1025 °C, —heating up to 1550 °C, —heating up to 1470 °C.

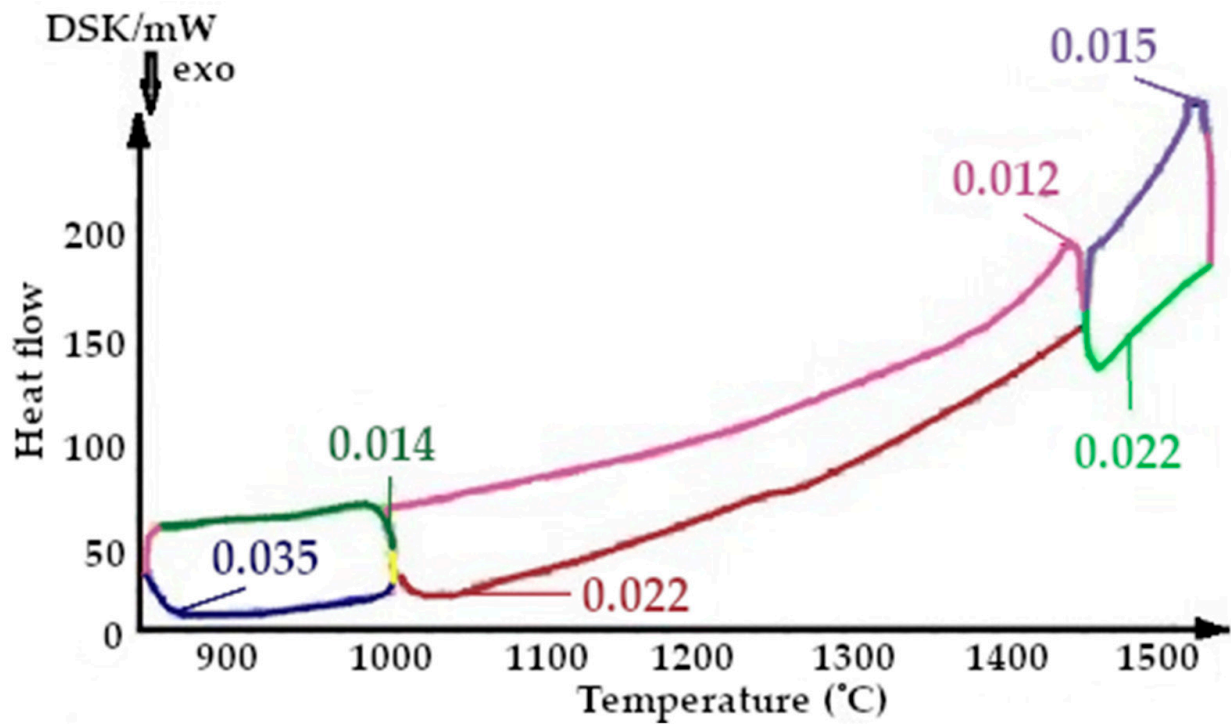


Figure 13. Fragment of the thermogram of quartzite, calcified at a temperature of 200 °C (Cycle 3), where: —cooling up to 1470 °C, —drainage at 1025 °C, —heating up to 1025 °C, —cooling up to 1025 °C, —cooling at 1550 °C, —heating up to 1470 °C, —heating up to 1550 °C.

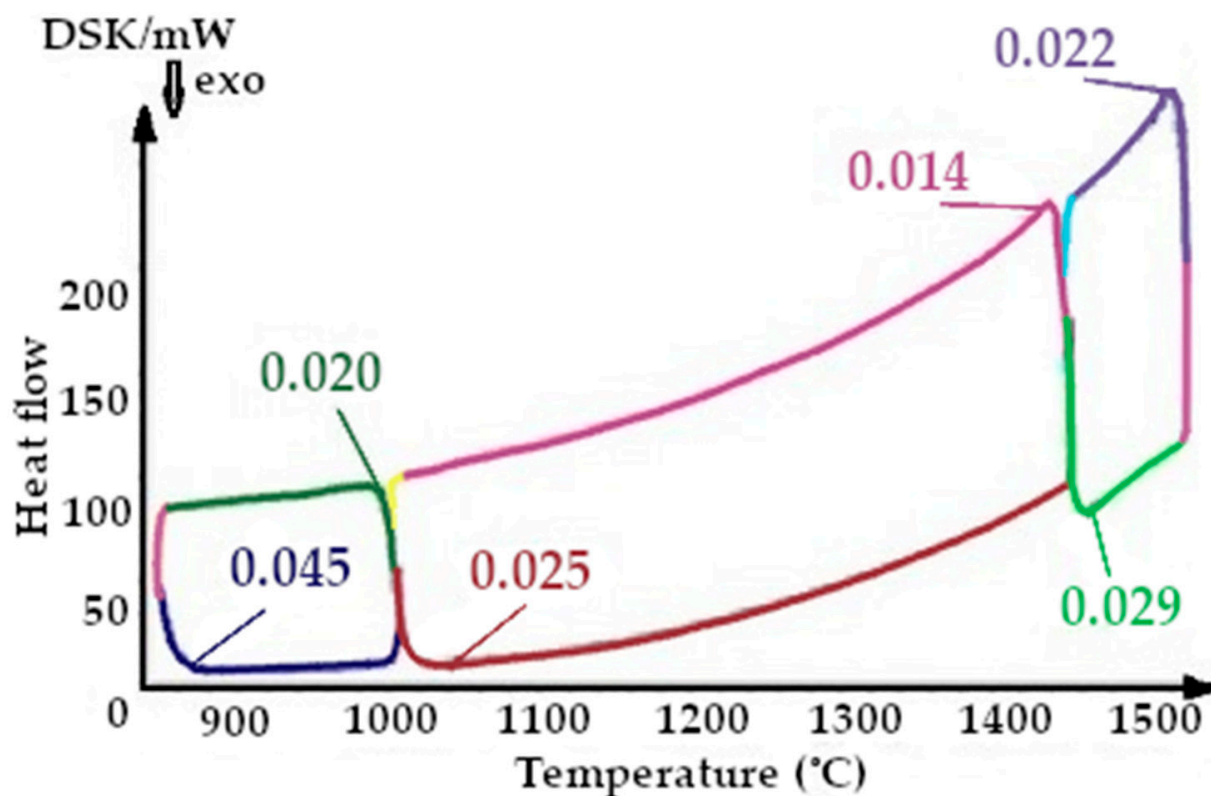


Figure 14. Fragment of the thermogram of quartzite, calcified at a temperature of 800 °C (Cycle 3), where: █—drainage at 800 °C, █—cooling up to 1470 °C, █—drainage at 1025 °C, █—heating up to 1025 °C, █—cooling up to 1025 °C, █—cooling at 1550 °C, █—heating up to 1470 °C, █—heating up to 1550 °C.

On the presented fragments of the first smelting cycle shown in Figures 9 and 10, it is evident that the heat capacity of the quartzite with pre-treatment of 200 °C is 2 times lower.

On the presented fragments of the second melting cycle, shown in Figures 11 and 12, it is evident that the heat capacity of the quartzite with a preliminary temperature treatment of 200 °C is 2.3 times lower.

On the presented fragments of the third melting cycle, shown in Figures 13 and 14, it is evident that the heat capacity of the quartzite with a preliminary temperature treatment of 200 °C is lower by 1.5 times.

All the thermograms have different colors for the cooling and heating periods during imaging.

In addition, based on the thermograms shown in Figures 6 and 7, Table 5 of the enthalpy values for the studied quartzites has been compiled.

Studies have found that, despite the presence of 0.638% impurities in the quartzite, its preliminary calcination at a temperature of 800 °C and further cooling allowed the process of further sintering of the chalcedony lining based on it. At 1550 °C, we simultaneously obtained the following three phases: hexagonal quartzite + tridymite + cristobalite. Its structure consisted of elementary cells corresponding to 82% of the tridymite phase, 9% of cristobalite and 9% of hexagonal quartzite, and it had an average volume of V_{av} of 1606.96 Å³ (Table 3).

The resulting enthalpy graph showed that at this point, the heat absorption process of the sintered layer exceeded the heat absorbed into the next lining layer by 72%. During subsequent melting cycles, the fraction of tridymite increased and thus the average volume also increased, and the heat transfer process began to exceed its absorption by 1.5- to 4-fold (Figure 15). The heat capacity graph shows that after sintering, the heat capacity of the liner

(ΔC_p) was 0.037 J/K, and in subsequent melting cycles, it was characterized by λ -shaped jumps of between 0.05 and 0.045 J/K (Figure 8).

Table 5. The enthalpy values of quartzites at the operating temperatures of melting cycles. No. 1, quartzite treated at 200 °C; No. 2, quartzite treated at 800 °C.

Enthalpy	Temperature (°C)													
	Cooling		Heating		Cooling		Heating		Cooling		Heating			
	1550–1470	1470–1025	1025–870	870–1025	1025–1470	1470–1550	1550–1470	1470–1025	1025–870	870–1025	1025–1470	1470–1550	1550–1470	1470–1025
Quartzite No. 1 (mJ/g)	2263	1117	61	−57	−333	−1406	2235	763	234	−171	−369	−1322	2187	1781
Quartzite No. 2 (mJ/g)	1947	1680	75	−122	−228	−1402	446	604	57	−43	−322	−2462	1749	1459

Based on these data, a graph of the changes in the enthalpy of quartzites is shown in Figure 15.

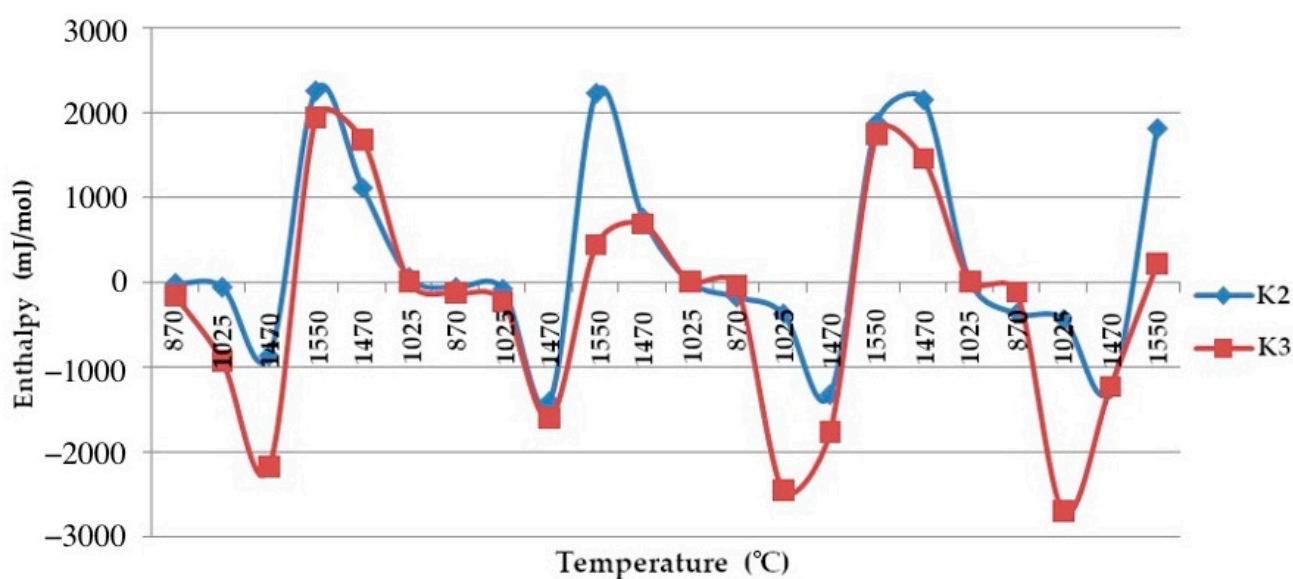


Figure 15. The enthalpy–temperature graph. ■—Quartzite treated at a temperature of 800 °C; ■—quartzite treated at a temperature of 200 °C.

After completion of the sintering mode of the lining at 1550 °C, the structure of the quartzite pre-processed at 200 °C consisted of elementary cells. The corresponding phases were 26% cristobalite and 74% hexagonal quartzite and had an average volume of 143.65 Å³ (Table 3). The resulting enthalpy graph shows that at this point, the heat absorption process of the sintered layer exceeded the heat absorbed into the next lining layer by 62%. In subsequent melting cycles, the fraction of cristobalite increased, and thus, the average volume also increased, and the absorption process is 59% (second cycle) and 57% (third cycle). The heat capacity graph shows that after sintering, the heat capacity of the liner (ΔC_p) was 0.018 J/K; in subsequent melting cycles, the liner was characterized by λ -shaped jumps of between 0.04 and 0.02 J/K (Figure 8).

The results of the changes in the heat capacity of the quartzite with different temperature treatments are shown in Figures 9–14. Of these, it can be seen that the quartzite with a

temperature treatment of 200 °C, after each cycle, the heat capacity is significantly lower than when processing 800 °C.

Thus, changes in the heat capacity and heat transfer and absorption were influenced by phase changes in the quartzite under the influence of temperature. Quartzite is known to be stable at 870–1470 °C, has a density of 2.3 g/cm³ and a hardness of 6.5 units on the Mohs scale. Cubic cristobalite is stable at a temperature of 1470–1715 °C, has a hardness of 7.25 units and has a density of 2.27 g/cm² [51]. The greater hardness of the lining makes it more resistant to intense melting movement at elevated melting temperatures.

Based on this technology, in the foundry of a machine-building enterprise equipped with industrial frequency induction smelters of 1 and 2.5 tons, the process of smelting synthetic iron on one steel scrap was developed, including the manufacture of the lining itself with reference to existing equipment. Work during the month showed a positive result—the resistance of the lining on all p-hours was 320–340 melts. Based on this, the technology was adopted as the main one, and the results during the year showed that the resistance of the lining on the smelting furnaces, stable, amounted to 320–360 melts. An analysis of the use of raw materials was carried out and compared with the previous technology. For metal filling containing 30% of steel scrap, the following materials were purchased: 15% (150 kg) of cast iron at 40 rubles/kg at 6000 rubles; 1% (10 kg) of ferro-manganese and ferrosilization at 50 rubles/kg at 500 rubles; 30% (300 kg) steel scrap at a price of 10 rubles/kg in the amount of 3000 rubles and 0.6% (0.6 kg) carburizer at a price of 3 rubles/kg in the amount of 1.8 rubles.

The rest of the metal residue consisted of the return of production and the liquid residue in the kiln, the notional cost of 1 ton, which is 50% for the liquid residue and for the return of 80% SCH20 (Grey Cast Iron, GG-20 in Germany)—70 rubles/kg ($330 \cdot 35 = 11,500$ rubles and $200 \cdot 56 = 11,200$ rubles).

The total cost amounted to 32,201.8 rubles/t liquid. For the smelting of 1 ton of liquid, when used in the meteor mill 88% of steel scrap, the costs amounted to the following: 1.5% ferrosile in the amount of 750 rubles; 100 kg liquid residue at the price of 5000 rubles; 88% of scrap steel in the amount of 8800 rubles and 2% carburizer in the amount of 6 rubles. The total cost of buying fresh materials amounted to 14,556 rubles. The calculation uses the market value of the materials as of 2018–2019.

5. Conclusions

According to these results, the sintered lining layer consisting of cristobalite and hexagonal quartzite, compared with a similar layer consisting mainly of tridymite, had a smaller average volume, its heat capacity at 1550 °C during the second and third melting cycles was 1.2–2 times lower, and the heat absorption process exceeded the heat transfer from the sintered to the semi-finished layer by 50%. In a sintered layer consisting of tridymite and quartzite, the process of heat transfer exceeded its absorption by 1.5–4 times, resulting in a more intensive change in the structure of the layers by accelerating the conversion of the half-melted material into filaments. This reduced the thickness of the lining, speeding up wear and thus reducing its durability.

Thus, research has shown that the acid lining, which has a lower heat capacity, has a higher hardness and, therefore, increased resistance to the intense movement of the melt, which will allow it to maintain its high resistance at melting temperatures up to 1470–1570 °C. This ensures the possibility of use in metal filling 90% or more, one steel scrap, reduces material and energy costs and increases productivity by reducing the downtime associated with the furnace. Based on the results of the research, the technology for manufacturing such a lining has been developed and proposed, including the main operations described below.

For the operation of removing moisture from the original raw material, it is necessary to make it use a temperature of 200 °C with subsequent cooling. The sintering process must be finished at a temperature of 1550–1570 °C with an exposure of 2 h. The first 3–5 melts

are carried out with 1/3 of the capacity of the crucible and only then go to the necessary melting mode.

In this way, the efficiency of using a sheet consisting of quartzite and cristobalite, which has a low heat capacity, allows the use of metal filling with 88% of steel scrap and provides a 45.2% reduction in the cost of raw materials.

Author Contributions: Conceptualization, V.A.K., V.V.K., V.S.T. and S.O.K.; methodology, V.A.K., V.V.K., V.S.T. and S.O.K.; validation, S.V.T., I.A.P., R.B.S., S.V.E. and T.A.P.; formal analysis, V.A.K., S.V.T., I.A.P., S.V.E. and T.A.P.; investigation, V.S.T., S.O.K., R.B.S., S.V.T. and S.V.E.; resources, V.A.K., V.V.K., V.S.T. and I.A.P.; data curation, V.A.K., V.V.K., V.S.T., S.O.K. and S.V.T.; writing—original draft preparation, V.A.K., V.V.K., V.S.T., S.O.K., R.B.S., S.V.T., I.A.P., S.V.E. and T.A.P.; writing—review and editing, V.A.K., V.V.K., V.S.T., S.O.K., R.B.S., S.V.T., I.A.P., S.V.E. and T.A.P.; visualization, V.A.K., V.V.K., R.B.S., S.V.T. and I.A.P.; supervision, V.S.T., S.O.K., S.V.E. and T.A.P.; project administration, V.A.K., V.S.T. and S.O.K.; All authors have read and agreed to the published version of the manuscript.

Funding: This research received no external funding.

Institutional Review Board Statement: Not applicable.

Informed Consent Statement: Not applicable.

Data Availability Statement: Not applicable.

Conflicts of Interest: The authors declare no conflict of interest.

References

- Chisamera, M.; Stan, S. Enhanced Quality in Electric Melt Grey Cast Irons Iulian Riposan. *ISIJ Int.* **2017**, *53*, 1683–1695.
- Gandhewar, V.R.; Bansod, S.V.; Borade, A.B. Induction furnace—A review. *Int. J. Eng. Technol.* **2011**, Volume 3, pp. 277–284.
- Luzgin, V.I.; Petrov, A.Y.; Fatkullin, S.M.; Koptiyakov, A.S.; Bolotin, K.E.; Shvydkiy, E.L. Energy-Efficient Induction Furnaces for the Production of Synthetic Cast Iron. *Proc. XII Congr. Foundry Work. Russ.* **2015**, *1*, 343–349.
- Kulkarni, U.; Wali, U. Power Efficiency Tracking of Induction Furnaces. In Proceedings of the 2020 IEEE International Conference on Electronics, Computing and Communication Technologies, Bangalore, India, 2–4 July 2020; pp. 1–4.
- Kukartsev, V.V.; Antamoshkin, O.A. Combined Method of Decision-Making on Reproduction of Fixed Production Assets. *Probl. Mech. Eng. Autom.* **2011**, *2*, 56–60.
- Onigbajumo, A.; Seidu Salio, O.; Akinlabi, O.; Newton, I. Melting Time Prediction Model for Induction Furnace Melting Using Specific Thermal Consumption from Material Charge Approach. *J. Miner. Mater. Charact. Eng.* **2021**, *9*, 61–74.
- Futas, P.; Pribulova, A.; Petrik, J.; Pokusova, M.; Junakova, A. The Study of Synthetic Cast Iron Quality Made from Steel Scrap. In Proceedings of the 18th International Multidisciplinary Scientific GeoConference SGEM 2018, Albena, Bulgaria, 20 June 2018.
- Shumikhin, V.S.; Luzan, P.P.; Zelnis, M.V. *Synthetic Cast Iron*; Naukova dumka: Kiev, Ukraine, 1971.
- Edalati, K.; Akhlaghi, F.; NiliAhmadabadi, M. Influence of SiC and FeSi Addition on the Characteristics of Gray Cast Iron Melts Poured at Different Temperatures. *Mater. Proc. Technol.* **2005**, *160*, 183–187. [[CrossRef](#)]
- Golubtsov, V.A. About the Situation in the Domestic Foundry Production. *Foundry Prod.* **2011**, *1*, 2–3.
- Kukartsev, V.A.; Trunova, A.I.; Kukartsev, A.V. Thermal Analysis of Quartzite Used to Line a Crucible-Equipped Industrial-Frequency Induction Furnace. *Refract. Ind. Ceram.* **2014**, *55*, 220–222. [[CrossRef](#)]
- Kaibicheva, M.N. Properties of Quartzite Masses Used for Lining Induction Furnaces of Large Capacity. *Refractories* **1971**, *4*, 31–33.
- Kaibicheva, M.N. Lining of Induction Furnaces in Germany and Other Capitalist Countries. *Refractories* **1970**, *3*, 52. [[CrossRef](#)]
- Sassa, V.S. *Lining of Induction Melting Furnaces and Mixers*; Energoatomizdat: Moscow, Russia, 1983.
- Ananiev, Y.S.; Ananyeva, L.G.; Dolgov, I.V.; Korobeinikov, A.F.; Korovkin, M.V. Search, Evaluation and Enrichment of Quartz Raw Materials for High Technologies. *Bull. Tomsk Poly-Tech. Univ.* **2001**, *304*, 123–130.
- Sokolov, D.Y.; Baranov, A.N. Silicon—The Main Element of the Development of Solar Energy. *Actual Probl. Humanit. Nat. Sci.* **2016**, *1*, 21–22.
- Naumova, O.V.; Mavzovin, V.M.; Chesnokov, B.P. Obtaining Silicon for Solar Cells from Mineral Raw Materials. *Tech. Regul. Transp. Constr.* **2020**, *43*, 320–332.
- Nepomnyashchikh, A.I.; Krasin, B.A.; Vasilyeva, I.E.; Eliseev, I.A.; Eremin, V.P.; Fe-doseenko, V.A.; Sinitskiy, V.V. Silicon for Solar Energy. *Bull. Tomsk. Polytech. Univ. Geo-Resour. Eng.* **2000**, *303*, 176–190.
- Zavertkin, A.S. Development of Lining from Karelian Quartzites for Crucible Induction Furnaces. *Refract. Ceram.* **2009**, *50*, 400–405. [[CrossRef](#)]
- Shishkin, G.A.; Marchenko, A.A.; Ivanov, N.A. Investigations of the Properties and Possibilities of Using Quartzite of the 0–20 Mm Fraction of the Cheremshansky Deposit. *Bull. Irkutsk State Tech. Univ.* **2012**, *64*, 78–85.
- Nelub, V.; Gantimurov, A.; Borodulin, A. Economic Analysis of Data Protection in Systems with Complex Architecture Using Neural Network Methods. *Econ. Ann.* **2020**, *185*, 178–188. [[CrossRef](#)]

22. Strelkov, K.K. *Technology of Refractories*; Metallurgy: Moscow, Russia, 1978.
23. Turchaninov, V.S. *Interaction of Refractories with Metals and Slags*; VIO: Lenindrad, Russia, 1978.
24. Kukartsev, V.A. Application of Pervouralsky Quartzite in Acid Lining for Induction Cast Iron Furnaces. *Foundry Russ.* **2012**, *1*, 35–37.
25. Platonov, B.P.; Akimenko, A.D.; Bogutskaya, S.M. *Induction Furnaces for Melting Cast Iron*; Energy: Moscow, Russia, 1976.
26. Kukartsev, V.A.; Kukartsev, V.V.; Kukartsev, A.B. Influence of thermal treatment of quartzite on the stability of the lining of industrial frequency induction crucible furnaces. *New Refract.* **2018**, *5*, 28–33.
27. Kassie, A.; Assfaw, B. Achamyeh. Minimization of Casting Defects IOSR. *J. Eng.* **2013**, *3*, 31–38.
28. Zuno-Silva, J.; Bedolla-Jacuinde, A.; Martínez-Vázquez, J.M.; Pérez-Perez, A.; Quintero-Azuara, T. Laboratory scale study of uncommon degradation SiO₂ refractories used on induction furnaces. *Nova scientia.* **2014**, *6*, 113–134. [[CrossRef](#)]
29. Fenner, C.N. The Various Forms of Silica and Their Mutual Relations. *Was. Acad. Sei* **1912**, *1*, 471–480.
30. Wahl, F.M.; Grim, R.E.; Graf, R.B. Phase Transformations in Silica as Examined by Continuous X-ray Diffraction. *Uniaersitl Illinois. Urbana Illinois. Am. Mineral.* **1961**, *46*, 196–208.
31. Thompson, A.B. Heat Capacities and Inversions in Tridymite, Cristobalite, and Tridymite-Cristobalite Mixed Phases. *Am. Mineral.* **1979**, *64*, 1013–1026.
32. Kukartsev, V.A.; Kukartsev, V.V.; Kukartsev, A.V. Effect of the Temperature Treatment of Quartzite on the Lining Resistance of Commercial-Frequency Induction Crucible Furnaces. *Refract. Ind. Ceram.* **2018**, *59*, 252–256. [[CrossRef](#)]
33. Denice, D.; Arya, A.; Kumar, M.; Vinod, G. First-principles study of electronic, cohesive and elastic properties of silica polymorphs. *Mater. Today Commun.* **2022**, *31*, 103607. [[CrossRef](#)]
34. Palmer, D.C.; Finger, L.W. Pressure-induced phase transition in cristobalite: An X-ray powder diffraction study to 4.4 GPa. *Am. Mineral.* **1994**, *79*, 1–8.
35. Ringdalen, E. Changes in Quartz during Heating and the Possible Effects on Si Production. *JOM* **2015**, *67*, 484–492. [[CrossRef](#)]
36. Pryanishnikov, V.P. *System of Silica*; Publishing House of Literature on Construction: Leningrad, Russia, 1971.
37. Novakovicr, R.; Radicr, S.M.; Risticr, M.M. Kinetics and Mechanism of Quartz-Tridymite Transformation. *Interceram* **1986**, *35*, 29–30.
38. Sanmoy, M. Kinetics of Quartz Transformation. *Indian Ceram. Soc.* **2014**, *1*, 25–38.
39. Shchiptsov, V.V.; Perepelitsyn, V.A.; Grishenkov, E.E.; Enenko, V.P.; Zavertkin, A.S. Pervoural'skii and Karel'skii Quartzites for The Lining of Crucible-Type Induction Furnaces. *Refract. Ind. Ceram.* **2003**, *44*, 67–74. [[CrossRef](#)]
40. Florke, O.W. Quartz, cristobalite and tridymite. *Silikattechnik.* **1961**, *12*, 304–305.
41. Nikiforova, E.M.; Eromasov, R.G.; Simonova, N.S.; Vasilyeva, M.N.; Taskin, V.Y. Phase Transformations in the Siliceous Rocks-Mineralizer System. *Mod. Probl. Sci. Educ.* **2012**, *1*, 218–219.
42. Zhang, H.; Guo, S.; Wu, J.; Wu, D.; Wei, K.; Ma, W. Effect of Quartz Crystal Structure Transformations on the Removal of Iron Impurities. *Hydrometallurgy* **2021**, *204*, 105715. [[CrossRef](#)]
43. Swainson, I.P.; Dove, M.T.; Palmer, D.C. Infrared and Raman spectroscopy studies of the α - β phase transition in cristobalite. *Phys. Chem. Miner.* **2003**, *30*, 353–365. [[CrossRef](#)]
44. Zavertkin, A.S. Effect of Quartzite Heat Treatment on Induction Furnace Lining Failure Mechanism. *Refract. Ind. Ceram.* **2019**, *60*, 67–70. [[CrossRef](#)]
45. Slovikovskii, V.V.; Gulyaeva, A.V. Effective linings for Kivcet furnaces. *Refract. Ind. Ceram.* **2014**, *54*, 350–352. [[CrossRef](#)]
46. He, J.; Jusnes, K.F.; Tangstad, M. Phase Transformation in Quartz at Elevated Temperatures. *Metadata Show Full Item Rec. Collect. Inst. Mater.* **2021**, *1*, 691–699.
47. Vettegren, V.I.; Mamaliev, R.I.; Sobolev, G.A. Blurred Phase Transition in a Quartz Surface Layer under Temperature Change. *Solid State Phys.* **2013**, *55*, 1987–1992. [[CrossRef](#)]
48. Kukartsev, V.A.; Abkarian, A.K.; Kukartsev, A.V. Investigation of the Influence of the drying Temperature on the Change in the Interplane Distances of the Crystal Lattice and the Properties of Pervouralsky Quartzite Used in the Compositions of the Lining Masses Of Induction Furnaces by X-ray Methods. *Refract. Tech. Ceram.* **2014**, *2*, 16–23.
49. Kukartsev, V.A.; Trunova, A.I.; Kukartsev, A.V. Thermal Analysis of Quartzite Used for Lining of an Industrial Frequency Induction Crucible Furnace. *New Refract.* **2014**, *1*, 33–35.
50. Topor, N. *Thermal Analysis of Minerals and Inorganic Compounds*; Moscow State University: Moscow, Russia, 1987.
51. Li, W.; Xu, C.; Xie, A.; Chen, K.; Yang, Y.; Liu, L.; Zhu, S. Microstructure Study of Phase Transformation of Quartz in Potassium Silicate Glass at 900 °C and 1000 °C. *Crystals* **2021**, *11*, 1481. [[CrossRef](#)]

Disclaimer/Publisher's Note: The statements, opinions and data contained in all publications are solely those of the individual author(s) and contributor(s) and not of MDPI and/or the editor(s). MDPI and/or the editor(s) disclaim responsibility for any injury to people or property resulting from any ideas, methods, instructions or products referred to in the content.